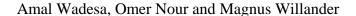# Linköping University Post Print

The effect of the interlayer design on the electroluminescence and electrical properties of n-ZnO nanorod/p-type blended polymer hybrid light emitting diodes

Amal Wadesa, Omer Nour and Magnus Willander

N.B.: When citing this work, cite the original article.

The effect of the interlayer design on the electroluminescence and electrical properties of n-ZnO-nanorods/p-blended polymer hybrid light emitting diodes

A. Wadeasa[1,*], O. Nur[1], and M.. Willander[1,2,*]

[1]Department of Science and Technology, Campus Norrköping,

Linköping University, SE-601 74 Norrköping, Sweden

[2]Department of Physics, Gothenburg University, SE-412 96 Gothenburg, Sweden

*Corresponding Author: amawa@itn.liu.se, magwi@itn.liu.se

Abstract

Hybrid light emitting diodes (LEDs) based on n-ZnO nanorods and blended polymers were fabricated and characterized. The blended polymers consisted of a blue emitting polymer and a charge transport polymer. The effect of the interlayer design on the electrical and electroluminescent characteristics of these hybrid LEDs was investigated. We demonstrated that by adding a Calcium (2) acetylacetonate [$Ca(acac)_2$] layer between the blended polymer layer and the ZnO nanorods, an increase in device performance was observed. The purpose of the extra layer was to act as a band offset stepping layer (offset divider). Moreover, the effect of the stepper layer thickness for this offset stepping layer was studied. The results indicate that LED performance is greatly affected by the presence and thickness of this band offset stepping layer.

Key words: ZnO-nanorods, p-type polymer, LEDs.

PACS: 62.23.Hj, 87.85.Rs, 62.23.Pq, 81.07.-b.

1. Introduction

Researchers have spent decades trying to create novel optoelectronic devices with light emitting diodes (LEDs) as the main focus. Since the 1960s, research in inorganic LEDs of different colors has been ongoing, including red, green, and blue. These multi-colored LEDs are already on the market, and their use is widespread in traffic lights, automotive brake signals displays, car lights and other applications. Among inorganic materials ZnO is currently considered as one of the most attractive electroluminescent materials for research on possible future lighting sources. This is mainly due to its unique properties, such as: wide direct band gap (3.4 eV), large exciton binding energy (60meV), commercial availability of large-area ZnO substrates and the possibility of performing wet etching. However, the fabrication of high quality, low resistivity and reproducible p-type ZnO has not yet been achieved. Hence the fabrication of stable ZnO p-n homo-junction based LEDs remains an unaccomplished goal [1-5].

On the other hand, organic semiconductors have proven to provide stable p-type electrodes, and different organic light emitting diodes (OLEDs) based on organic semiconductors have been demonstrated [6-7]. Nowadays LEDs based on organic semiconductors are available in the market for different purposes. But n-type polymers are limited to a very small number of molecules and polymers. This is because the availability of polymers with n-type conductivity is low due to some problems, such as difficulty in synthesis, poor solubility and poor stability in air [6-8]. Moreover, blended polymer solutions have been used in OLEDs for a long time [9]. By blending the emissive material, charge transport properties are enhanced and photoluminescent (PL) efficiency is usually increased. This allows more degrees of freedom in the choice of materials and the optimization of each of the single processes involved in electroluminescence (EL) [10]. Their advantages are also combined with strong enhancement in electroluminescence (EL) efficiency when compared to pure homo-polymers, as expected [11].

Combining n-ZnO-nanorods and p-type blended polymers in hybrid structure LEDs will open the way to a new class of LEDs that can emit in a wide range of the visible spectrum. Hence, this could lead to the development of efficient white light LEDs. There have been few published reports on ZnO-nanorods/organic light emitting diodes, examples of these can be found in [12-14]. To the best of our knowledge no report has dealt with blended polymer emissive layers and only single un-blended polymers have been used to demonstrate inorganic-organic hybrid LEDs.

In this paper, we demonstrate a hybrid n-ZnO nanorod/p-type blended polymer light emitting diode (LEDs) using low temperature and cheap growth techniques. The device shows high intensity emission and covers most of the visible range. The effect of adding Calcium (2) acetylacetonate [Ca(acac)$_2$] layer, which functions as a hole divided/electron blocking layer, is investigated. In addition, the dependency of the current density on the thickness variation of the Ca(acac)$_2$ layer has been studied.

2. Experimental details

For all devices, glass was used as a substrate after being cleaned with acetone, iso-propanol and de-ionized water. Silver metal (Ag) was evaporated using thermal evaporation to provide a bottom contact. Poly(3,4ethylenedioxythiophene) poly(styrenesulfonate) (PEDOT: PSS) was spun coated to a layer thickness of 60nm. Poly (9, 9-dioctylfluorene) (PFO) [8, 12] and Poly (9, 9-dioctyl-fluorene-co-N(4 butylphenyl) diphenylamine) (TFB) [15] were blended in toluene acid and spun coated to produce a 376nm thick layer. Calcium (2) acetylacetonate (Ca(acac)$_2$) [16] (see figure 1(a)), was dissolved in de-ionized water and added on the top of the blended polymer film for a 33nm film thickness. A calcium (2) acetylacetonate layer was used as a step progression from the HOMO level at the polymer side to the valence band of ZnO. As can be seen in the equilibrium energy band schematic diagram (figure 2 (a) and (b)) [16-19], the energy level difference (offset) between the blended polymer HOMO and the ZnO valence band is divided into two parts when comparing the two cases (with or without the interfacial layer). It is expected that this will enhance the emission properties as more holes will flow to the n-type side of the junction. Specifically, the

emission taking place at the ZnO part of the junction is expected to be enhanced. The ZnO-nanorods were then grown on the top of the previous layers for five hours using the aqueous chemical growth (ACG) method as described in reference [20]. Finally, gold (Au) was thermally evaporated to make the top contact. All parameters were the same for all devices (spin speed, spin time and growth time, etc.) and all measurements were carried out in air at room temperature. Film morphology and thickness were investigated using scanning electron microscopy (SEM) and DEKTAK 3ST Surface Profile measurement. The electrical characterization of the diode was measured using an electrical parameter analyzer HP4540. The photoluminescence (PL) and electroluminescence (EL) measurements were performed at room temperature using an Andor-Newton DU-970N CCD camera. For PL measurements a Nd:YAG laser source with 280 nm excitation wavelength was used. The higher energy detection limit was adjusted to 400 nm during EL and PL measurements.
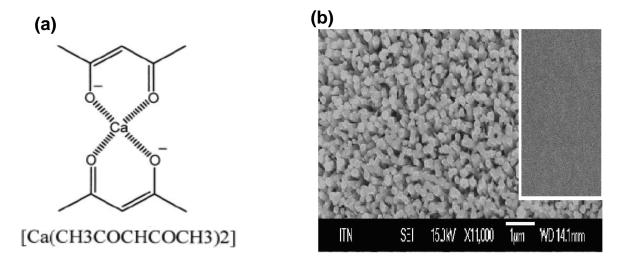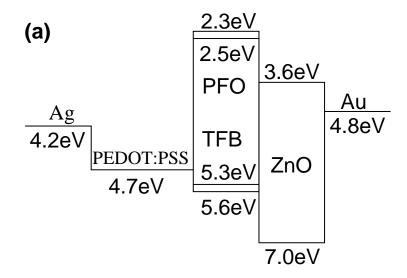

Figure 1. *(a) The chemical structure of the Ca(acac)$_2$ material.*
(b) The morphology of the ZnO-nanorods grown on the top of (PEDOT: PSS-TFB-PFO-Ca(acac)$_2$) layers. The insert in the right side of the figure shows the morphology of these layers (PEDOT: PSS-TFB-PFO- Ca(acac)$_2$) before ZnO-nanorods growth.

(a)

2.3eV

2.5eV

PFO

3.6eV

Au

4.8eV

Ag

4.2eV

PEDOT:PSS

TFB

5.3eV

ZnO

4.7eV

5.6eV

7.0eV

(b)

2.3eV 2.4eV

2.5eV

PFO

3.6eV

Au

4.8eV

Ag

4.2eV

PEDOT:PSS

TFB

5.3eV

$Ca(acac)_2$
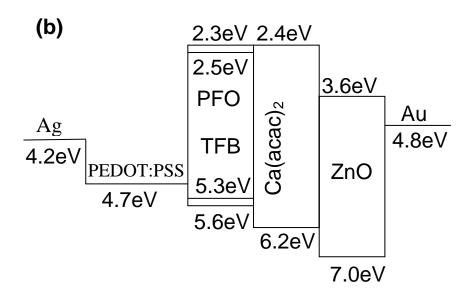
ZnO

4.7eV

5.6eV

6.2eV

7.0eV

Figure 2. The equilibrium energy-band diagram of the hybrid LEDs (a) without the $Ca(acac)_2$ layer and (b) with a layer of the $Ca(acac)_2$.

3. Results and discussion

3.1. Morphology and equilibrium band diagram

Film morphology, after spinning of the PEDOT: PSS layer and the blended polymer film, shows high uniformity as shown in the insert fig. 1(a). The uniformity of the surface is an important factor for the subsequent growth of the nanorods. A typical SEM of the final ZnO-nanorods grown at low temperature on top of the polymer is shown in figure 1(b) as can be seen; the resulting ZnO-nanorods obtained are dense, vertical (in average) and relatively long. The diameter and length of the nanorods were about 110nm and 1.74µm, respectively. Figure 2 shows the equilibrium energy band diagram for the LEDs with and without a Ca(acac)$_2$ layer. The highest occupied molecular orbital (HOMO) and lowest unoccupied molecular orbital (LUMO) energies are extracted from the literature [16-19]. The HOMO of the PEDOT: PSS and the valance band of the ZnO values were checked experimentally using Ultra-violet photoemission spectroscope (UPS) technique (results not shown here). Our PEDOT: PSS material shows a HOMO with a value of 4.7eV and most of the demonstrated publications shows that the HOMO value lies between 5.0 - 5.4 eV [21]. The low HOMO value in our case is probably due to the aging of the PEDOT: PSS used. Nevertheless, this is not expected to affect the initial film morphology or device functionality as the PEDOT: PSS film is used as a hole injection layer. Instead, our new value (4.7eV) gives the opportunity to have the same energy offset (1.2 eV) from the metal to the injection layer(s) in both sides (see figure 2). For the configuration without the Ca(acac)$_2$ layer (figure 2(a)) we observe the following: (i) the HOMO level of the blended film (5.5eV) is much higher than the valance band of the ZnO (7.0eV) leading to a confinement of the holes within the blended layer; (ii) The conduction band of ZnO (3.6eV) is much lower than the LUMO of the polymer blend layer (2.4eV) (iii) as electrons have higher density and mobility in ZnO compared to the blended polymers [22], they will accumulate on the polymer blend layer and most of the emission will originate from the polymer side. By adding the Ca(acac)$_2$ layer (figure 2(b)), the energy difference between the LUMO level of the Ca(acac)$_2$ layer and the polymer blended layer will not change, but the energy difference between the HOMO level of the blended polymer and the ZnO valence band will be divided into two small energy barriers. The introduction of this band offset divider is expected to enhance hole injection to

the ZnO side of the junction. This will in turn affect the luminescence intensity and the ZnO contribution in the spectrum of the whole device (confirmed by I-V, PL and EL spectra).

3.2. Current–voltage characteristic

Figure 3((a) and (b)) show the room temperature I-V characteristics of both configurations (with and without the $Ca(acac)_2$ layer). The I-V characteristics revealed very good rectifying diode-like behavior. This implies the presence of a good p-n heterojunction between n-ZnO nanorods and the p-type blended polymer. The nature of the current-voltage characteristics was analyzed as follows: first the injection limiting current (ILC) is detected due to the high offset (0.5eV) between the metal and the PEDOT: PSS layer, followed by an ohmic regime appearing at low voltage (< 1V) with the slope (S=1) indicating a good ohmic contact as shown in the insert of fig. 3(a), then, when in the region of higher voltage (> 1V), we have observed that (S=2), which implies the presence of trap-free space-charge-limited current regime, which follows the Mott-Gurney formula [23]. At even higher bias (> 4V) the slope become steep (< 3). This region corresponds to the trap-filling regime due to rapid change undergone by the current as the Fermi level, E_F, moves through a trap level, E_t [23]. The threshold voltage was equal to 2.5V and the breakdown voltage was found to be -13V. After adding the $Ca(acac)_2$ layer, as clearly seen in figure 3(a), the total current is increased. The current density at (6V) was found to be equal to (4.5mA/cm^2) for the device without the $Ca(acac)_2$ layer and equal to (9.46 mA/cm^2) for the device with the $Ca(acac)_2$ layer. The observed current enhancement in this case corresponds to a 100% increase. The insertion of the $Ca(acac)_2$ layer did not change the threshold voltage but the breakdown voltage was increased to -30V as shown in figure 3(c). Furthermore, the leakage current was measured at -15V for both configurations. For the device without the $Ca(acac)_2$ layer the current density was found to be 1.69 mA/cm^2 and after adding the $Ca(acac)_2$ layer it become 0.009 mA/cm^2 as shown in figure 3(c). This implies that better current balance was achieved by adding the $Ca(acac)_2$ layer, as expected. Figure 4 shows the effect of an increase in the $Ca(acac)_2$ layer thickness on the current density of the LEDs. Curve 1 in figure 4 shows the device without the
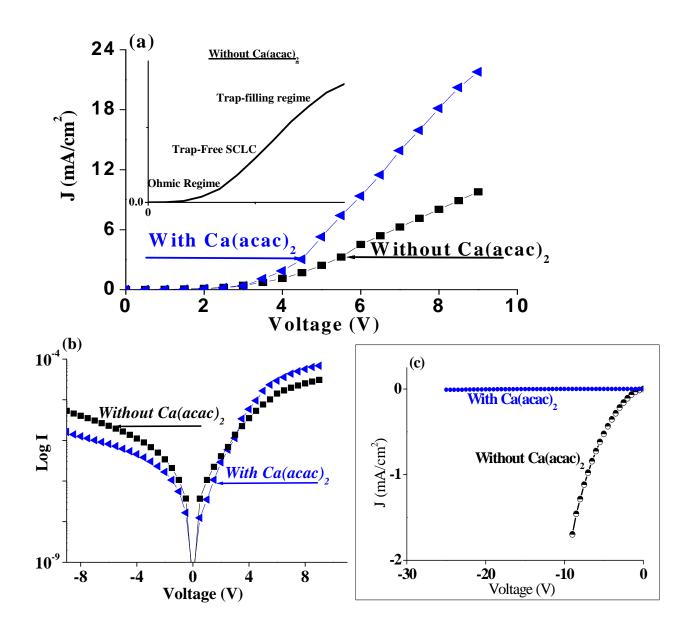
Figure 3. *The current density versus voltage characteristics for:*
(a) The LEDs without and with the Ca(acac)₂ layer. The insert in the right side of the figure shows different current regime, (b) The logarithmic scale of the current versus voltage for the same devices and (c) The leakage current diagram for the device in the reverse bias direction for both configurations, with and without the Ca(acac)₂ layer.

Ca(acac)$_2$ layer and the other curves, 2-6, are for the same configuration with different Ca(acac)$_2$

thicknesses. At the beginning, the current density increases with an increase of the Ca(acac)$_2$ layer

thickness until it approaches a saturation value at a thickness of about 2.13µm (curve 3). After this

thickness the current density starts to decrease. Also, curve 4 (5.03µm) shows fast decrease in the current density as compared to curve 3 (2.13µm). This is due to the increase in the thickness of the $Ca(acac)_2$ layer, so we expect that after the saturation the rapid increase in $Ca(acac)_2$ layer thickness will increase the resistance of the device which will lead to the observed drop in the current density value.
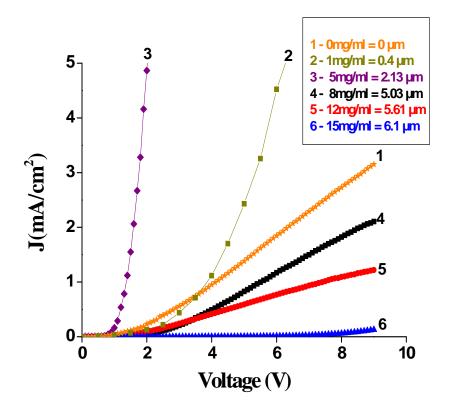

Figure 4. The current density versus applied forward bias characteristics of the hybrid LED with different Ca(acac)$_2$ layer thicknesses.

3.3. Photoluminescence

Figure 5 shows the PL spectra for the LEDs with or without the $Ca(acac)_2$ layer. Both devices show two main peaks; the first peak has a maximum intensity centered at 504 nm, which
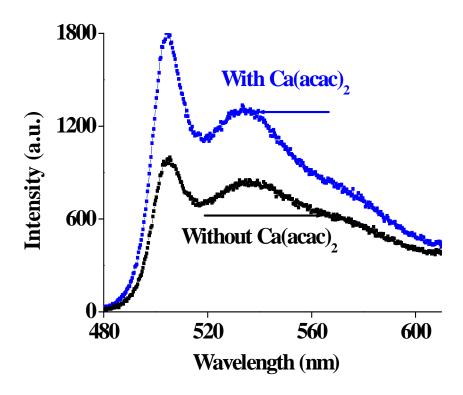
9

Figure 5. PL spectrums using Nd: YAG laser source with (280nm) excitation wave length for the LED devices for both configurations, with and without the Ca(acac)₂ layer.

belongs to the PFO emission and is assigned to emission from excimers or aggregates [24]. The second peak has maximum intensity centered at around 533nm and belongs to the deep band emission (DBE) from ZnO. This peak (533nm) is attributed to the radiative recombination of a photo generated hole in the valence band with an electron occupying a deep oxygen vacancy level [25]. For the configuration with the $Ca(acac)_2$ layer, no shift in the peak positions for the PFO or ZnO materials was observed. The only difference was the enhancement in the intensity (55% increases) for the device with the $Ca(acac)_2$ layer when compared to the other device. Although we expect that it is due to change in the defect amount and distribution at the interface zone, the exact reason for the enhancement in the PL emission is not clear and is under further investigation.

3.4. Electroluminescence

        The EL spectra of the present devices are shown in figure 6 for both configurations (with and without the $Ca(acac)_2$ layer). The PFO peak was detected with maximum intensity centered at 456nm. Some authors, such as K. Sakamoto et al., attribute this peak to excitonic emission and its vibronic progression from non interacting single chains [26]. Another broad peak centered at 510nm was detected, which represents the DBE of the ZnO material. Two more peaks were detected, the first one, with a maximum intensity centered at 561nm, originates from the transition between the conduction band and the zinc vacancies, [27] the second one has lower intensity and is centered at 640nm. This peak originates from oxygen interstitials and belongs to the orange-band emission [28]. This EL spectrum was measured at 16V and the corresponding current value was 0.005mA. When the $Ca(acac)_2$ layer was inserted, no change in the PFO polymer peak position was observed. A broad green emission with a peak which has a maximum intensity centered at around 540nm was detected. This peak belongs to the oxygen vacancies [29]. In addition, the intensity was increased 400% in the device with the $Ca(acac)_2$ layer as compared to the device without the layer, as shown in figure 6. By adding the $Ca(acac)_2$ layer which will divide the hole energy barrier between the ZnO valance band and the HOMO of the blended layer into two small barrier, see figure 2 the amount of the holes injected to the interface layer will increase and the charge carrier balance (hole and electron) will be improved. This will increase the exciton formation and recombination probability in general.
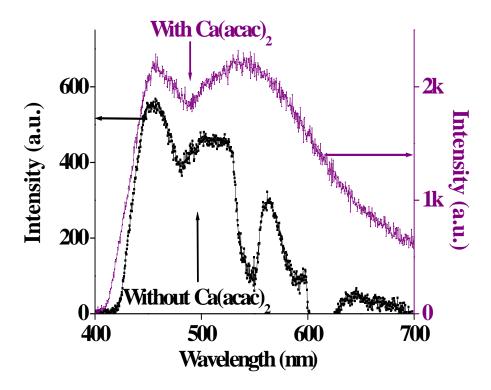
Figure 6. *EL spectrums for the LED devices for both configurations, with the Ca(acac)$_2$ layer and without it.*

4. Conclusions

To sum up, based on cheap and low temperature growth methods, preferentially oriented ZnO-nanorods were grown on top of smooth p-type blended polymer layers on a glass substrate. We demonstrate that by adjustment of the design of the polymer layers, it is possible to increase the luminescence by up to 400% compared to reference LEDs. This is achieved by choosing a layer that provides better stepping of the band offsets between the ZnO valence band and the polymer HOMO level. Specifically, the effect of adding a Ca(acac)$_2$ layer on LED performance was investigated. The results show that by adding a Ca(acac)$_2$ layer the current density was doubled

and the emission spectra intensity was increased by a factor of four for TFB/PFO-ZnO LEDs. In addition, when using this stepping layer the breakdown voltage of the hybrid LED from -13V to -30V. The effect of the layer thickness shows that the improvement of the LED performance saturates at a specific thickness corresponding to 2.13µm. For a thickness greater than this the current density starts to drop. Light emitting diodes with this hybrid structure provide broad emission electroluminescence devices ranging from 410 nm up to nearly 700 nm. The LEDs presented here covered the blue, green and orange emission ranges and hence provide a possibility of producing white light sources.

References

[1] Chen Q C and Zhu J 2007 Appl. Phys. Lett. **90**, 043105.

[2] Lucas M, Mai W, Yang R, Wang L Z, and Riedo E 2007 Nano Lett. **5**, 1314.

[3] Al-Hilli S, Öst A, Strålfors P, and Willander M 2007 J. Appl. Phys. **102**, 084304.

[4] Zhao X Q, Klason P, Willander M, Zhong M H, Lu W and Yang H J 2005 Appl. Phys. Lett. **87**, 211912.

[5] Klason P, Borseth M T, Zhao X Q, Svensson G B, Kuznetsov Y A, Bergman J P and Willander M 2008 Solid State Comm. **145**, 321.

[6] Bernius T M, Inbasekaran M, O`Brien J, and Wu W 2000 Adv. Mater. **12**, 1737.

[7] Morgado J, Friend H R, Cacialli F 2002 Appl. Phys. Lett. **80**, 14.

[8] Redecker M, Bradley C D D, Inbasekaran M and Woo P E 1998 Appl. Phys. Lett. **73**, 1565.

[9] Moon E 2002 Condens. Matter **14**, 12235.

[10] Campbell J A et.al. SPIE 2002 4464 (ed.Kafafi Z. H.) 211-222 (SPIE, Washington, 2002).

[11] Chappell J, Lidzey G D, Jukes C P, Higgins M A, Thompson L R, O`Connor S, Grizzi I, Flecher R, O`Brien J, Geoghegan M and Johanes L A R 2003 Nature **2**, 616.

[12] Könenkamp R, Word R and Schlegel C 2004 Appl. Phys. Lett. **85**, 24.

[13] Chang C, Tsao F, Pan C and Chi G 2006, Appl. Phys. Lett. **88**, 173503.

[14] Meyer J, Görrn P, Hamwi S, Johannes -H H, Riedl T and W. Kowalsky W, 2008 Appl. Phys. Lett. **93**, 073308.

 [15] Tsami A, Yang –H X, Galbrecht F, Farrell T, Li H, Adamczyk S, Heiderhoff R, Balk J L, Neher D and Holder E 2007 Polymer Chemistry **45**, 4773.

 [16] Kambe E, Ebisawa A, Shirai S and Shinkai M 2003 Extended Abstracts, The 50th Spring Meeting, The Japan Society of Applied Physics and Related Societies, p. 1405.

[17] Tsami A, Yang X-Hui, Galbrecht F, Farrell T, Li H, Adamczyk S, Heiderhoff R, Balk J L, Neher D and Holder E 2007 J. Polymer. Sci. A, **45**, 4773.

[18] Ryu Y S, Jo J S, Kim S C, Choi H S, Noh H J, Baik K H, Jeong S H, Han W D, Song Y S, and Lee S K 2007 Appl. Phys. Lett, **91**, 093515.

 [19] Wan S A, Mäkinen J A, Lane A P, Kushto P G 2007 J. Chem. Phys. Lett. **446**, 317.

[20] Vayssieres L 2003 Adv. Mater. **15**, 464.

[21] A. D. Pasquier, D. D. T. Mastrogiovanni, L. A. Klein, T. Wang, and E. Garfunkel, Appl. Phys. Lett. **91**, 183501(2007).

[22] Klason P 2008 Zinc Oxide Bulk and Nanorods, Ph. D. thesis ISBN 978-91-628-7492-6 Gothenburg University, Sweden.

[23] Carbone A, Kotowska K B, and Kotowski D 2005 Phy. Rev. Lett. **95**, 236601.

[24] Neher D 2001 Macromol. Rapid Commun. **22**, 13366.

[25] Børseth Moe T, Svensson G B and Kuznetsov Yu A, Klason P, Zhao X Q, and Willander M 2006 Appl. Phys. Lett. **89**, 262112.

[26] Sakamoto K, Usami K, Uehara Y, Ushioda S 2005 Appl. Phys. Lett **87,** 211910.

[27] Heo W Y, Norton P D, Pearton J S 2005 J. Appl. Phys. **98**, 073502.

[28] Wu L X, Siu G G, Fu L C and Ong C H 2001 Appl. Phys. Lett. **78**, 2285.

[29] Özgür Ü, Alivov I Y, Liu C, Teke A, Reshchikov A M, Doˇgan S, Avrutin V, Cho –J S and Morkoç H 2005 J. Appl. Phys. **98**, 041 301.